

Analysis and simulation of dynamic properties for the DFB laser

Abstract. The numerical analysis of dynamic properties of the distributed feedback laser (DFB) is presented. The model is based on coupled rate equations, which can describe mutual relations between a photon number, an electron number and an optical phase in the active region of the DFB laser. The presented numerical approach includes intrinsic fluctuations of laser parameters and laser noises caused by these fluctuations to the model using the fourth order Runge-Kutta method. The DFB model can be consequently applied for a purpose of advanced simulations performed in the complete optical transmission model.

Streszczenie. Zaprezentowano analizę numeryczną właściwości dynamicznych lasera typu DFB. Model bazuje na sprzężonych równaniach opisujących wzajemne relacje między liczbą fotonów, liczbą elektronów i fazą optyczną części aktywnej lasera. W modelowaniu wykorzystano metodę Runge-Kutta czwartego rzędu. W opracowanym modelu uwzględniono możliwość fluktuacji parametrów lasera i wynikające stąd szумы. **Analiza i symulacja właściwości dynamicznych lasera typu DFB**

Keywords: the DFB laser, laser rate equations, output characteristics, the Runge-Kutta algorithm, numerical simulations.

Słowa kluczowe: laser typu DFB, algorytm Runge-Kutta, właściwości dynamiczne

Introduction

Constantly increasing end-user requirements lead to increased demands for the data transmission speed and thus to the need to develop new technologies used in optical transmission networks. Recently, the focus has been paid to the transmission systems with capacity in excess of 100 Gb.s⁻¹ per one channel [1]. This amount of capacity can be only reached using high order modulation formats, multiplexing techniques, such as the wavelength division multiplexing (WDM), the spatial division multiplexing (SDM), and high-quality optical sources with a very narrow spectral linewidth [1-4]. Laser noises [5-7] are one of the most limiting factors of the optical transmission system. Therefore, it is necessary to create a model of the DFB laser that can represent behavior of the light source including its limitations. The DFB laser model must be based on measured parameters in order to predict its corresponding system performance. In general, the intent of creating an optical transmission system model is important for testing optical modulation and/or coding techniques, noise thresholds, etc. [8-9]. In this paper, the complete numerical approach used in a simulation model for the DFB laser is presented, as improvement in existing optical transmission system developed before [10-11]. Laser output characteristics as the electron number, the photon number, the optical phase, the optical power and laser noises caused by fluctuations of these characteristics are obtained as results from the laser rate equation model based on parameters extracted by I. Fatadin and his team in [12]. We propose a mathematical methodology that can be used to model the DFB laser's behavior under different operating conditions. In the Section I., the laser rate equation model including noise fluctuations is introduced. In the Section II., results of numerical simulations are presented and, finally, a conclusion of our work is situated.

I. The Laser Rate Equation Model

The inner dynamics of DFB lasers can be modelled by a set of rate equations, which describe the interaction between photons and electrons inside the active region with added extra noise term, known as the Langevin noise source. This equation model is originally derived from Maxwell's equations [13].

$$(1) \quad \frac{dS(t)}{dt} = \left(g \frac{N(t)-N_0}{1+\epsilon S(t)} - \frac{1}{\tau_p} \right) S(t) + \frac{\beta N(t)}{\tau_n} + F_S(t)$$

$$(2) \quad \frac{dN(t)}{dt} = \frac{I(t)}{q} - \frac{N(t)}{\tau_n} - g \frac{N(t)-N_0}{1+\epsilon S(t)} S(t) + F_N(t)$$

$$(3) \quad \frac{d\Phi}{dt} = \frac{\alpha}{2} g (N(t) - \bar{N}) + F_\Phi(t)$$

The rate equations can be obtained heuristically by taking into account physical phenomena through which the number of electron N and the number of photons S change with time inside the active region, as illustrated in fig.1.

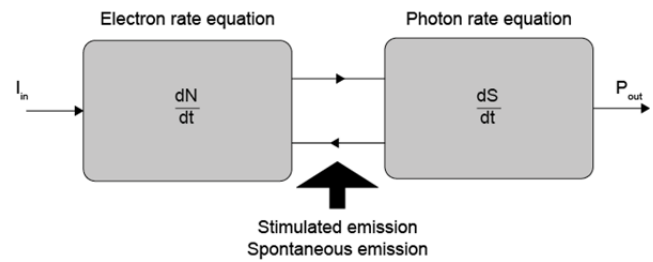


Fig.1. The single-mode laser model expressed by the rate equation

Equations (1) – (3) represent laser rate equations for a single-mode laser. These rate equations are used to compute simulation of the photon number $S(t)$, the electron number $N(t)$ and the optical phase $\Phi(t)$. Parameters of these rate equations are presented in Table 1.

Table 1. Extracted parameters used in rate equations

Parameter name	Parameter
gain slope constant coefficient	g
carrier density at transparency	N_0
gain compression factor	sp
photon lifetime	τ_p
spontaneous emission coupled into lasing mode	β
injection current	$I(t)$
electron charge	q
electron lifetime	τ_n
group velocity	v_g
linewidth enhancement factor	α
time-averaged carrier number	\bar{N}

In the rate equations used above, the diffusion [5] and nonlinear effects [6] are lumped together as an effective field-dependent optical gain compression. This rather simple form is commonly employed by many authors [12–16]. The optical feedback [17] into laser is also not accounted by this model. However, the optical feedback

can be reduced experimentally by a sufficient optical isolation (15)

$$F_N(t) = F_Z(t) - F_S(t)$$

The fluctuation of the lasing frequency $\Delta\nu(t)$ is described by a variation of the optical phase as:

$$(4) \quad \Delta\nu(t) = \frac{1}{2\pi} \frac{d\Phi}{dt}$$

The random noise function in (1) - (3) representing intensity, phase and frequency fluctuations are caused by noise mechanisms (the spontaneous emission and the electron hole recombination). They are assumed to be the Gaussian process with zero mean value. Under the Markovian assumption, the correlation function of the form given by the Markovian approximation can be expressed as:

$$(5) \quad \langle F_i(t)F_j(t') \rangle = 2D_{ij}\delta(t-t')$$

where $i, j = S, N$ or Φ , δ is the Dirac's delta function angular, brackets denote the ensemble average, D_{ij} is called the diffusion coefficient and is listed as:

$$(6) \quad 2D_{SS} = \frac{2\beta N(t)S(t)}{\tau_n}$$

$$(7) \quad 2D_{NN} = \frac{2N(t)}{\tau_n} [1 + \beta S(t)]$$

$$(8) \quad 2D_{\Phi\Phi} = \frac{-2\beta N(t)S(t)}{\tau_n}$$

$$(9) \quad 2D_{SN} = \frac{-2\beta N(t)S(t)}{\tau_n}$$

Obtaining explicit forms for the functions $F_S(t)$, $F_N(t)$, $F_\Phi(t)$ is necessary due to numerical integration in (1) - (3). Unless these noise sources are cross-correlated, we could numerically simulate them with three independent random generations using their auto-correlations. Because of the cross-correlation between S and N in [18-19], the new variable $F_Z(t)$ can be defined as:

$$(10) \quad F_Z(t) = F_S(t) + F_N(t)$$

The noise functions $F_Z(t)$, $F_S(t)$ are mutually orthogonal without the cross-correlation between them so that we can define them independently and hence obtain $F_N(t)$ from (10). Then, the diffusion coefficient for variable F_Z can be expressed as follows:

$$(11) \quad 2D_{ZZ} = \frac{2N(t)}{\tau_n}$$

and appropriate noise sources can be expressed as:

$$(12) \quad F_S(t) = \sqrt{\frac{2D_{SS}(t)}{\Delta t}} x_s$$

$$(13) \quad F_\Phi(t) = \sqrt{\frac{2D_{\Phi\Phi}(t)}{\Delta t}} x_\Phi$$

$$(14) \quad F_Z(t) = \sqrt{\frac{2D_{ZZ}(t)}{\Delta t}} x_z$$

where x_s, x_Φ, x_z are three independent random numbers obtained from a Gaussian distribution with zero mean values and unity variances and Δt is the sampling time interval [19].

The optical output of the DFB laser is given by amount of emitting photons as follows:

$$(16) \quad p(t) = \frac{S(t)\eta_0 h\nu}{\tau_p}$$

where η_0 denotes the total differential quantum efficiency and $h\nu$ denotes the photon energy.

The threshold current of the DFB laser is given by:

$$(17) \quad I_{th} = \frac{qV_a}{\tau_n} \left[N_0 + \frac{1}{g\tau_p} \right]$$

II. Simulation Results and Discussion

All simulations are realized in Matlab R2017A. Two sets of simulation are computed to obtain output characteristics of the DFB laser. The first simulation is focused on steady-state characteristics as the L-I curve and the power dependency on the central lasing wavelength.

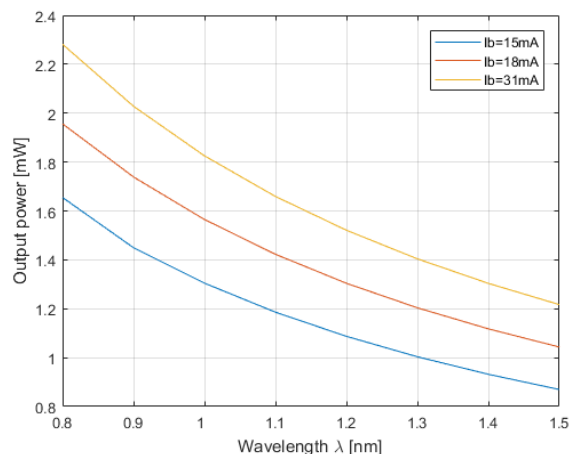


Fig. 2. Optical power dependencies on the central lasing wavelength for different bias currents

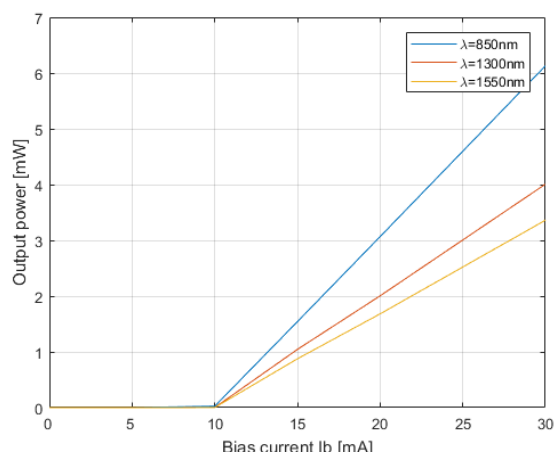


Fig. 3. Optical power dependencies on the input bias current for different wavelengths

In the fig.2, it can be seen how output power varies, when the central lasing wavelength is changed. In the fig.3, there are shown input-output characteristics (output power dependencies on the bias current) for three different central wavelengths.

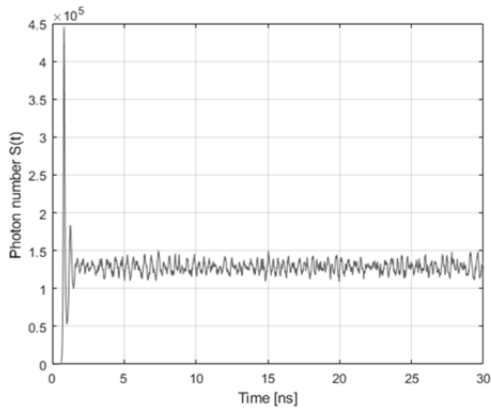


Fig. 4 Photon number fluctuations during the transient

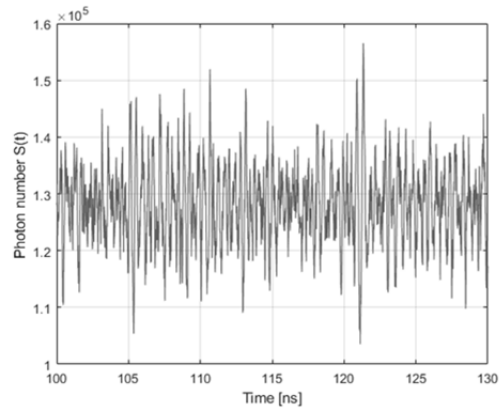


Fig. 8. Photon number fluctuations after the transient

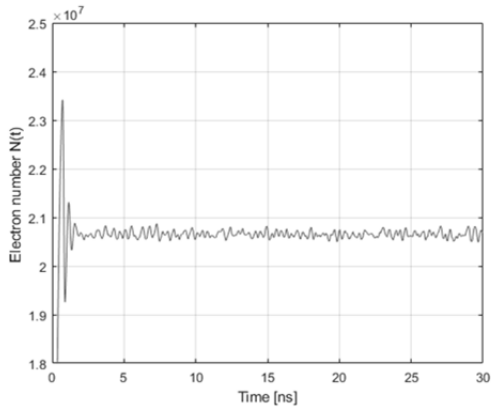


Fig. 5 Electron number fluctuations during the transient

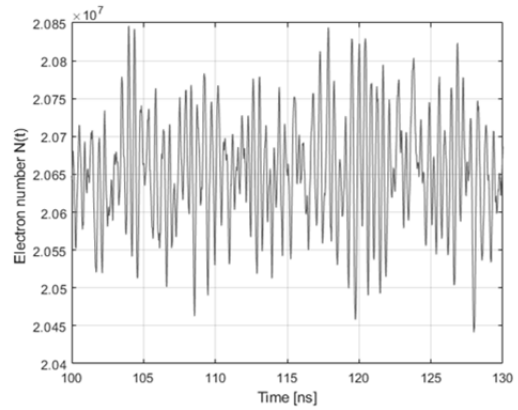


Fig. 9. Electron number fluctuations after the transient

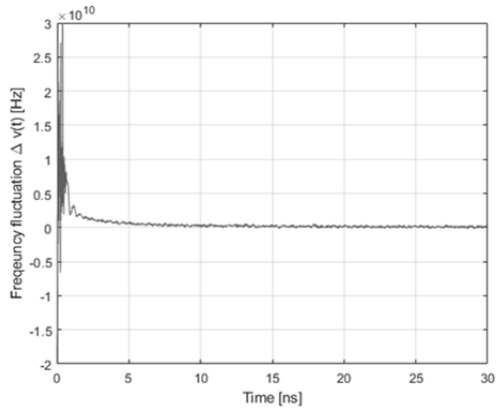


Fig.67 Central lasing frequency fluctuations during the transient

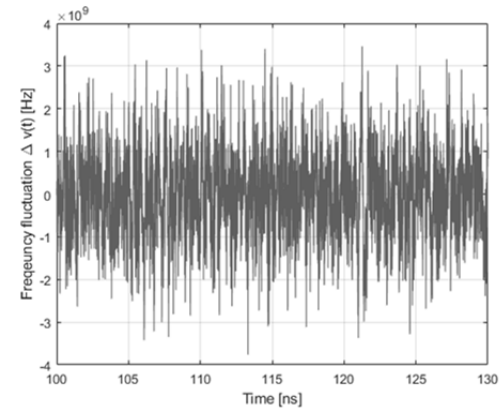


Fig. 10. Central lasing frequency fluctuations after the transient

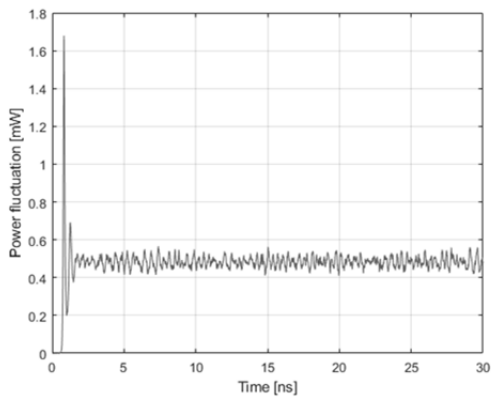


Fig. 7 Output power fluctuations during the transient

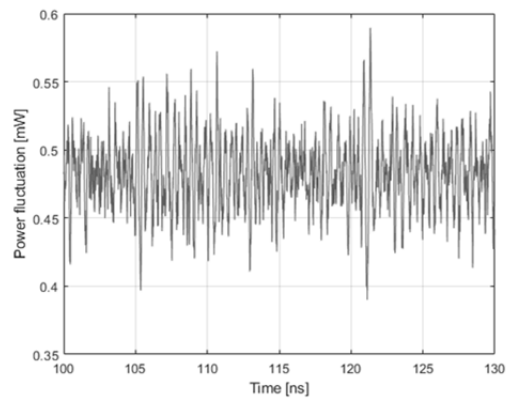


Fig. 11. Output power fluctuations after the transient

The second simulation is dedicated to the continuous wave lasing. Numerical results for output fluctuation characteristics are obtained using values of extracted parameters presented in Table 2. The fourth-order Runge-Kutta algorithm is used to compute the numerical integrations of (1) – (3). The time interval is set to $\Delta t = 10$ ps.

Table 2. Values of extracted parameters used in simulations

Parameter name	Parameter	Value
electron lifetime	τ_n	0.33×10^{-9} s
photon lifetime	τ_p	7.15×10^{-12} s
gain compression ratio	ϵ	4.58×10^{-8} m ³
carrier density at transparency	N_0	8.20×10^6 m ⁻³
spontaneous emission factor	β	3.54×10^{-5}
total differential quantum efficiency	η	0.21
central wavelength	λ	1550×10^{-9} m
gain slope constant coefficient	g	1.13×10^4 s ⁻¹

In fig.4 – 11, it can be seen time evolutions of the photon number $S(t)$, the electron number $N(t)$, the central lasing frequency fluctuation $\Delta\nu(t)$ and the output power fluctuation $P(t)$ during and after transients. The numerical simulations were performed with injection current $I = 12,9$ mA. Due to noise operators mentioned above, physical quantities are fluctuating around their steady state values. The noise operators are less visible during the start-up transient.

Conclusion

We have presented a detailed mathematical methodology in order to simulate a DFB laser's behavior using the laser rate equation model. The simulation is divided in two parts. The first part of simulation is focused on the steady-state approach, where L-I curves and wavelength dependencies can be obtained. The second part of simulation is devoted to the CW lasing. The presented steady-state equation model contains only values of parameters extracted from measurements. This approach can be also used to simulate a direct modulation of the DFB laser.

In the next contribution, this simulation will be compared to real DFB laser measurements. This DFB laser model is a component of the complete optical transmission system performed in Matlab R2017.

Acknowledgment

This work is a part of research activities conducted at Slovak University of Technology Bratislava, Faculty of Electrical Engineering and Information Technology, Institute of Multimedia Information and Communication Technologies, within the scope of projects VEGA agency project - 1/0462/17 "Modeling of qualitative parameters in IMS networks" and KEGA No. 007STU-4/2016 "Progressive educational methods in the field of telecommunications multiservice networks".

Authors: MSc. Pavol Šalík, Slovak University of Technology, Faculty of Electrical Engineering and Information Technologies Institute of Multimedia Information and Communication Technologies Ilkovičova 3, 81219 Bratislava, Slovakia, E-mail: pavol.salik@gmail.com;

Assoc. Prof. Ing. Rastislav Róka, PhD., Slovak University of Technology, Faculty of Electrical Engineering and Information Technologies Institute of Multimedia Information and Communication Technologies Ilkovičova 3, 812 19 Bratislava, Slovakia, E-mail: rastislav.roka@stuba.sk;

REFERENCES

- [1] Winzer P.J., "High-spectral-efficiency optical modulation formats," Journal of Lightwave Technology, vol.30, no.24, pp. 3824–3835, 2012.
- [2] Zeleny R., Lucki M., "Nearly zero dispersion-flattened photonic crystal fiber with fluorine-doped three-fold symmetry core," Optical Engineering, vol.52, no.4, Article ID045003, 2013.
- [3] Idachaba F., Ike D. U., Hope O., "Future trends in fiber optics communication," in Proceedings of the World Congress on Engineering, vol. I, pp. 2–6, 2014.
- [4] Litvik J., Kuba M., Benedikovic D., Dubovan J., Dado M., "Numerical estimation of spectral properties of laser based on rate equations," Mathematical Problems in Engineering, Volume 2016, Article ID 4152895, Hindawi, 2016
- [5] Mortazy E., Ahmadi V., Moravvej-Farshi K., "An integrated equivalent circuit model for relative intensity noise and frequency noise spectrum of a multimode semiconductor laser," IEEE J. Quantum Electr., vol.38, pp.1366-1371, October 2002.
- [6] Joindot I., "Measurements of relative intensity noise (RIN) in semiconductor lasers," Journal de Physique III, EDP Sciences, pp.1591-1603, 1992.
- [7] Urlick V.J., Devgan P.S., McKinney J.D., Dexter J.L., "Laser noise and its impact on the performance of intensity modulation with direct-detection analog photonic links," Naval research laboratory, DC 20375-5320, Washington, August 2007.
- [8] Róka R., Čertík F., "Simulation tools for broadband passive optical networks," in Simulation Technologies in Networking and Communications: Selecting the Best Tool for the Test. CRC Press, Taylor and Francis Group, pp. 337-364, 2015.
- [9] Čertík F., Róka R., "Possibilities for advanced encoding techniques at signal transmission in the optical transmission," Journal of Engineering – JE, vol.2016, Article ID 2385372, ISSN 2314-4904, March 2016.
- [10] Šalík P., Róka R., "Impact of environmental influences on multilevel modulation formats at the signal transmission in the optical transmission medium, Journal IJCNIS, vol.9, pp.76-87, ISSN 2076-0930, April 2017.
- [11] Šalík P., Čertík F., Róka R., "Duobinary modulation format in optical communication systems," Advances in Signal Processing, vol.3, no.1, pp.1-7, ISSN 2332-6883, 2015.
- [12] Fatadin I., Ives D., Wicks M., "Numerical simulation of intensity and phase noise from extracted parameters for CW DFB lasers," IEEE J. Quant. Electr., vol.42, no.9, pp.934–941, 2006.
- [13] Marcuse D., "Classical derivation of the Laser rate equation," IEEE J. Quantum Electr., vol.QE-19, no.8, 1983.
- [14] Binh L.N., "Optical Fiber Communications Systems: Theory and Practice with MATLAB® and Simulink® Models," Wiley-Interscience publication, ISBN 9781439806203, April 2010.
- [15] Tucker R., Pope D.J., "Circuit modeling of the effect of diffusion damping in a narrow-stripe semiconductor laser," IEEE J. Quantum Electr., vol.QE-19, pp.1179-1183, July 1983.
- [16] Tucker R., Kaminow I.P., "High-frequency characteristics of directly modulated InGaAsP ridge waveguide and buried heterostructure lasers," J. Lightwave Technology, vol.LT-2, no.4, pp.385-393, August 1984.
- [17] André P., Teixeira A., Pellegrino L.P., Lima M., Nogueira R., Monteiro P., Pinto A.N., Pinto J.L., and Rocha J.F.D., "Extraction of laser parameters for simulation purposes," NUSOD 2005, paper WP19, Berlin, Germany, 2005.
- [18] Ahmed M., Yamada M., Saito M., "Numerical modeling of intensity and phase noise in semiconductor lasers," IEEE J. Quantum Electr., vol.37, no.12, December 2001.
- [19] Šalík P., Róka R., "Analysis of Possibilities for Numerical Simulations of Continues Wave DFB Laser", ICUMT 2017 - 9th International Congress Munich, pp.215-219, ISBN 978-1-5386-3434-9, November 2017.